

Supporting Information

Highly Conducting Wurster-Type Twisted Covalent Organic Frameworks

Julian M. Rotter,^{a,‡} Roman Guntermann,^{a,‡} Michael Auth,^b Andre Mähringer,^a Andreas Sperlich,^b Vladimir Dyakonov,^b Dana D. Medina,^{a,*} Thomas Bein^{a,*}

^a*Department of Chemistry and Center for NanoScience (CeNS), University of Munich (LMU), Butenandtstrasse 5-13 (E), 81377 Munich, Germany*

^b*Experimental Physics VI, Julius-Maximilians-Universität Würzburg, 97074 Würzburg, Germany*

[‡]*These authors contributed equally to this work.*

Chemicals

All materials were purchased from Aldrich, Fluka, Acros or TCI Europe in the common purities purum, puriss or reagent grade. Materials were used as received without additional purification and handled under air unless noted. All solvents used were anhydrous and purged with inert gas.

Methods and Instruments

Nuclear magnetic resonance spectra were recorded on Bruker AV 400 and AV 400 TR spectrometers. Proton chemical shifts are expressed in parts per million (δ scale) and are calibrated using residual non-deuterated solvent peaks as an internal reference (e.g., DMSO-*d*₆: 2.50).

Powder X-ray diffraction measurements were performed on a Bruker D8 Discover diffractometer using Ni-filtered Cu K α radiation and a position sensitive LynxEye detector in Bragg-Brentano geometry.

Nitrogen sorption isotherms were recorded on a Quantachrome Autosorb 1 instrument at 77 K within pressure ranges of $p/p_0 = 0.001$ to 0.98. Samples for physisorption were directly taken from supercritical CO₂ activation. Prior to the measurements, the samples were heated for 12 h at 100 °C under high vacuum. For the evaluation of the surface area the BET method was applied within a p/p_0 range of 0.05 to 0.3. Pore size distributions

were calculated using the QSDFT absorption model with a carbon kernel for cylindrical pores.

Ultraviolet–Vis–infrared absorption spectra were recorded on a Perkin-Elmer Lambda 1050 spectrometer equipped with a 150 mm integration sphere.

Photoluminescence and time-correlated single photon counting measurements were carried out using a FluoTime 300 from PicoQuant GmbH. Samples were excited using a 378 nm laser source pulsed at 40 MHz and a fluence of 300 nJ cm⁻² / pulse.

Scanning electron microscopy images were recorded with an FEI Helios NanoLab G3 UC scanning electron microscope equipped with a field emission gun operated at 3 kV. Prior to the measurements, the samples were sputtered with carbon.

Transmission electron microscopy images were recorded with an FEI Titan Themis 60 - 300 equipped with a field emission gun operated at 300 kV.

Electrochemical measurements were performed on a Metrohm μ AutolabIII/FRA2 instrument using a three-electrode setup with a Pt-wire counter-electrode and a silver wire as a pseudo reference electrode under argon atmosphere. Measurements were carried out in dry acetonitrile with tetrabutyl ammonium tetrafluoro borate (1 M) as the electrolyte. After recording CV data, the measurement was repeated after a small amount of ferrocene was added to the sample. The position of the redox couple from Fc/Fc⁺ was then used as the reference system.

Van-der-Pauw measurements were carried out using an ECOPIA Model HMS 3000 setup. The samples were contacted with gold plated spring electrodes with an electrode separation of 5 mm. Powder pellets were pressed by using 20 mg of COF material and pressing into a cylindrical pellet with a circle diameter of 1 cm under a pressure of 8000 kPa.

Electron paramagnetic resonance (EPR)

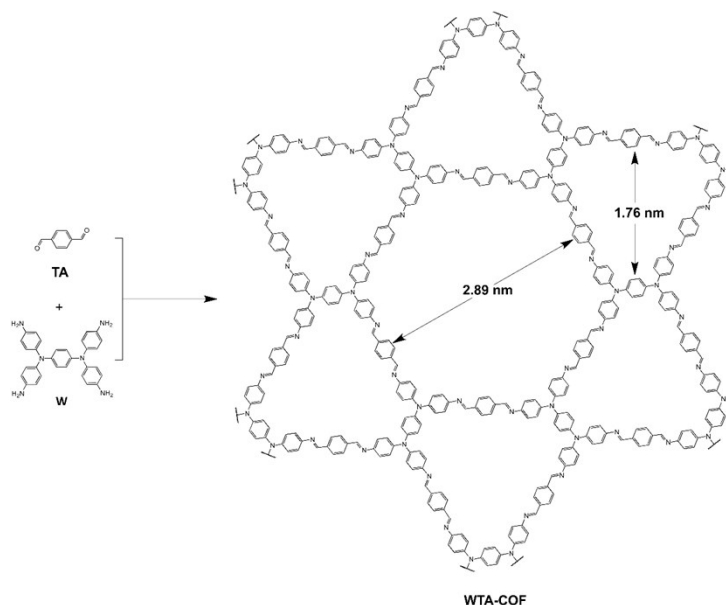
EPR was measured with a modified Bruker X-Band spectrometer (E300) in the dark at room temperature with a magnetic field modulation of 1 Gauss and microwave power set to 100 μ W (33 dB).

Theoretical Calculations

The initial structures of the COFs were built using the Forcite module of Accelrys Materials Studio 6.0 using the Universal Force Field as implemented. Pawley refinements were

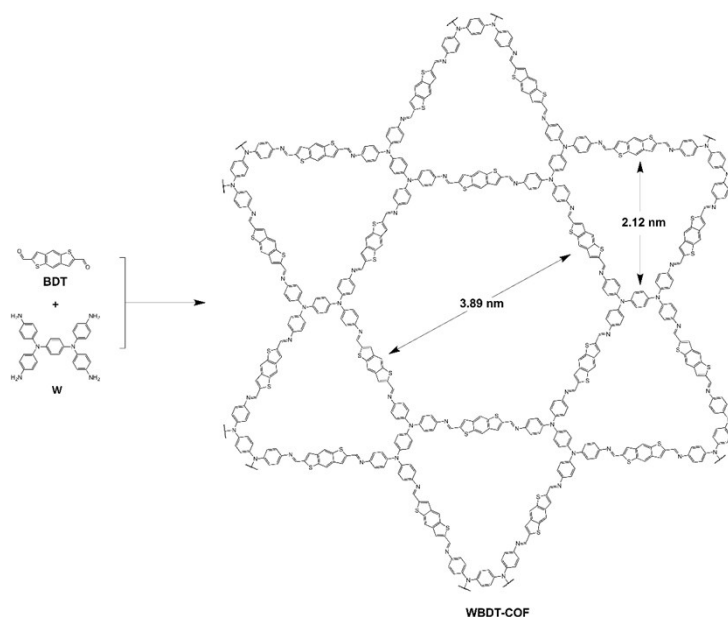
carried out using the Reflex module of PXRD with the Howard-profile fitting function. DFTB+ calculations were carried out using the DFTB+ code with the 3ob parameter set.¹ DFT calculations on the model pore systems were carried out using Gaussian 16 with the PBE0 functional and the def2SVP basis set with standard convergence criteria.

Synthesis of WTA



In a 5 mL culture tube, a solid mixture of terephthalaldehyde (**TA**, 0.025 mmol, 3.4 mg) and *N,N,N',N'*-tetrakis(4-aminophenyl)-1,4-phenylenediamine (**W**, 0.013 mmol, 6.0 mg) was suspended in 1 mL mesitylene and benzyl alcohol (1:1 V:V). The loading of the culture tube was carried out in an argon filled glovebox. Subsequently, 50 μ L of acetic acid (6 M) was added. Then, the culture tube was tightly sealed and heated at 100 $^{\circ}$ C for 72 h in an oven. The resulting dark red suspension was filtrated hot and the isolated powder was washed with 10 mL tetrahydrofuran (THF). The obtained red microcrystalline product was dried under vacuum and subsequently activated with supercritical CO₂ at 110 bar and 40 $^{\circ}$ C for 1 hour.

Synthesis of WBDT



In a 5 mL culture tube, a solid mixture of benzodithiophene-2,6-dicarboxaldehyde (**BDT**, 0.025 mmol, 6.26 mg) and *N,N,N',N'*-tetrakis(4-aminophenyl)-1,4-phenylenediamine (**W**, 0.013 mmol, 6.0 mg) was suspended in 1 mL mesitylene and benzyl alcohol (1:1 V:V). The loading of the culture tube was carried out in an argon filled glovebox. Subsequently, 50 μL of acetic acid (6M) was added. Then, the culture tube was tightly sealed and heated at 100 $^{\circ}\text{C}$ for 72 h in an oven. The resulting dark red suspension was filtrated hot and the isolated powder was washed with 10 mL tetrahydrofuran (THF). The obtained red microcrystalline product was dried under vacuum and subsequently activated with supercritical CO_2 at 110 bar and 40 $^{\circ}\text{C}$ for 1 hour.

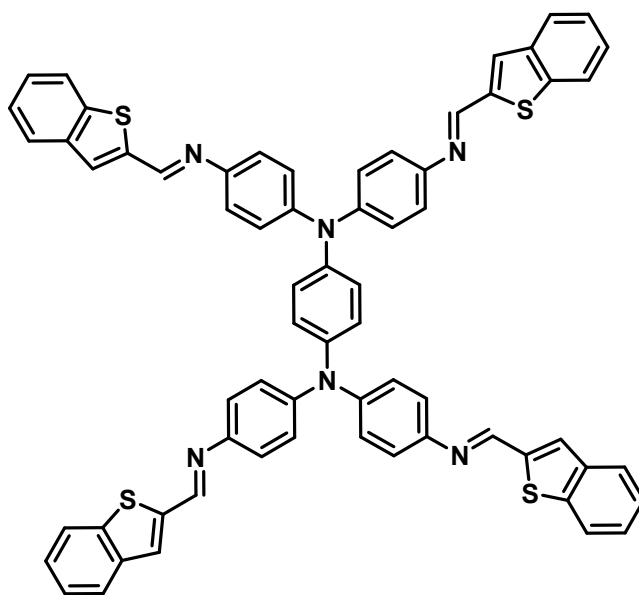
Synthesis of WTA thin films

In a 25 mL Schott duran glass bottle, a solid mixture of terephthalaldehyde (**TA**, 0.1 mmol, 13.6 mg) and *N,N,N',N'*-tetrakis(4-aminophenyl)-1,4-phenylenediamine (**W**, 0.052 mmol, 24.0 mg) was suspended in 4 mL mesitylene and benzyl alcohol (1:1 V:V). The loading of the reaction vessel was carried out in an argon filled glovebox. 200 μL of acetic acid (6 M) was added. A substrate holder with two horizontally oriented substrates (1.5 cm \times 1.5 cm) was placed into the suspension. The reaction vessel was tightly sealed and heated at 100 $^{\circ}\text{C}$ for 12 h in an oven. Then the substrate holder was taken from the vessel and the substrates from the holder. The upper sides of the substrates were cleaned from COF precipitates by wiping the surface with an acetone wetted cotton tip. Subsequently, the bottom sides of the substrates were washed with THF and dried under vacuum.

Synthesis of WBDT thin films

In a 25 mL Schott duran glass bottle, a solid mixture of benzodithiophene-2,6-dicarboxaldehyde (**BDT**, 0.1 mmol, 25.04 mg) and *N,N,N',N'*-tetrakis(4-aminophenyl)-1,4-phenylenediamine (**W**, 0.052 mmol, 24.0 mg) was suspended in 4 mL mesitylene and benzyl alcohol (1:1 V:V). The loading of the reaction vessel was carried out in an argon filled glovebox. 200 μ L of acetic acid (6M) was added. A substrate holder with two horizontally oriented substrates (1.5 cm \times 1.5 cm) was placed into the suspension. The reaction vessel was tightly sealed and heated at 100 $^{\circ}$ C for 12 h in an oven. Then the substrate holder was taken from the vessel and the substrates from the holder. The upper sides of the substrates were cleaned from COF precipitates by wiping the surface with an acetone wetted cotton tip. Subsequently, the bottom sides of the substrates were washed with THF and dried under vacuum.

Synthesis of the WBDT molecular fragment and single crystal growth

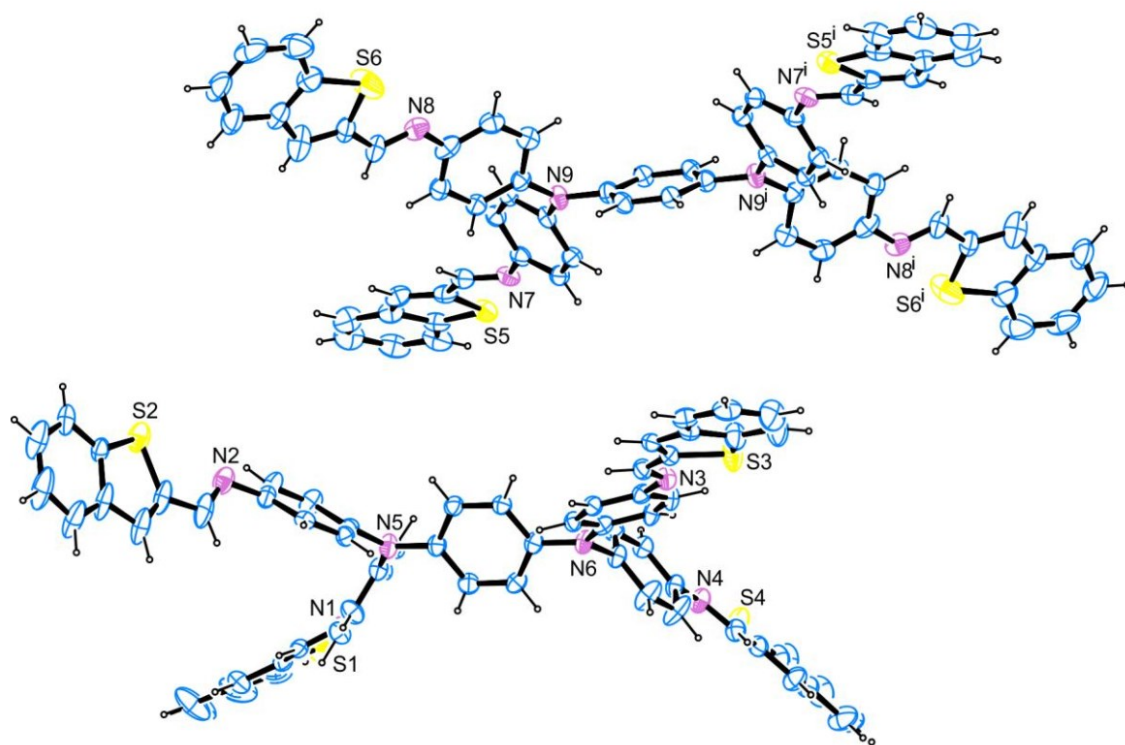


In a 5 mL culture tube, a solid mixture of benzothiothiophene-2-carboxaldehyde (0.25 mmol, 62.6 mg) and *N,N,N',N'*-tetrakis(4-aminophenyl)-1,4-phenylenediamine (**W**, 0.05 mmol, 23.0 mg) was suspended in 4 mL of CHCl_3 . The culture tube was sealed and heated for 24 h at 60 $^{\circ}$ C. Subsequently, the reaction was cooled to room temperature and the resulting precipitate was collected by filtration and washed with methanol (20 mL). The dark red material was dried under vacuum.

^1H NMR (400 MHz, $\text{DMSO-}d_6$) δ (ppm): 8.50 (4H), 7.79 (8H), 7.45 (8H), 7.32 (8H), 7.30 (4H), 7.18 (8H), 7.14 (4H).

MS-EI: calculated (m/z): $\text{C}_{66}\text{H}_{44}\text{N}_6\text{S}_4$ 1048.2510, found 1048.2478.

Single crystals were grown by dissolving 5 mg of the WBDT molecular fragment in dichloromethane (10 mL) in a 25 mL screw-capped vial equipped with a septum. A needle was pierced through the septum to allow for slow evaporation of the solvent at room temperature. After 5 days, red platelet-like crystals were obtained, which were removed from solution directly prior to single-crystal analysis.



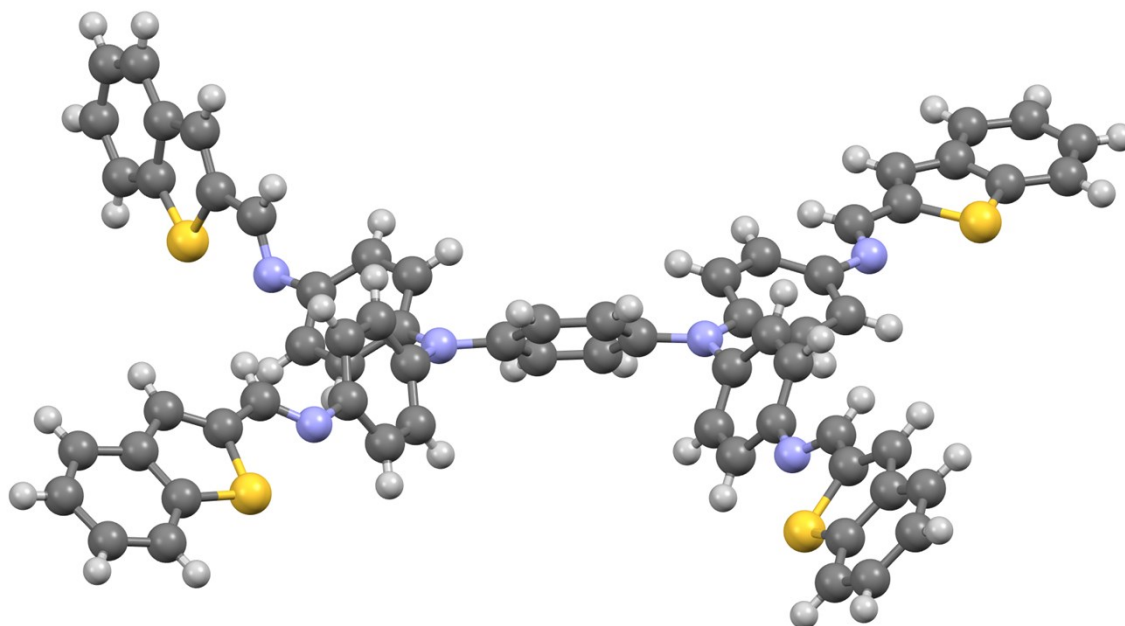


Figure S1: The molecular arrangement of the WBDT molecular fragment, obtained from single crystal data in ORTEP and stick-ball representation.

Table S1: Summary of the single crystal data of the WBDT molecular fragment.

net formula	$C_{67.55}H_{47.10}Cl_{3.09}N_6S_4$
$M_r/g\ mol^{-1}$	1180.73
crystal size/mm	$0.090 \times 0.070 \times 0.020$
T/K	106.(2)
radiation	Mo K_α
diffractometer	'Bruker D8 Venture TXS'
crystal system	triclinic
space group	'P -1'
$a/\text{\AA}$	13.8855(6)
$b/\text{\AA}$	17.9904(7)
$c/\text{\AA}$	19.1860(7)

$\alpha/^\circ$	77.1720(10)
$\beta/^\circ$	78.2210(10)
$\gamma/^\circ$	69.1000(10)
$V/\text{\AA}^3$	4324.4(3)
Z	3
calc. density/g cm ⁻³	1.360
μ/mm^{-1}	0.357
absorption correction	Multi-Scan
transmission factor range	0.96–0.99
refls. measured	58603
R_{int}	0.0538
mean $\sigma(I)/I$	0.0600
θ range	2.337–25.350
observed refls.	10556
x, y (weighting scheme)	0.1012, 10.3561
hydrogen refinement	Constr.
Refls. in refinement	15789
parameters	1321
restraints	406
$R(F_{\text{obs}})$	0.0811
$R_w(F^2)$	0.2308
S	1.023
shift/error _{max}	0.001
max electron density/e \AA^{-3}	1.274

min electron density/e \AA^{-3}

-1.050

There are several disordered parts in this structure. All methylene chloride molecules are disordered. Split models have been applied. SADI instructions have been used to restrain all C-Cl and all Cl-Cl distances to similar values. All but one of the CH_2Cl_2 moieties have been refined isotropically. The SIMU restraint has been used to refine the U_{ij} of adjacent atoms (to a distance of 0.8 \AA) similarly. The SAME instruction has been applied to obtain good bond geometries in two disordered branches of the macromolecules using well-refined branches as model. ISOR and FLAT restraints have been used to improve vibration ellipsoids and geometry, respectively.

The figure above does not show the methylene chloride molecules and the minor parts of disordered sections.

Symmetry code $i = 2-x, 1-y, 1-z$.

Simulated tetragonal structure of WTA

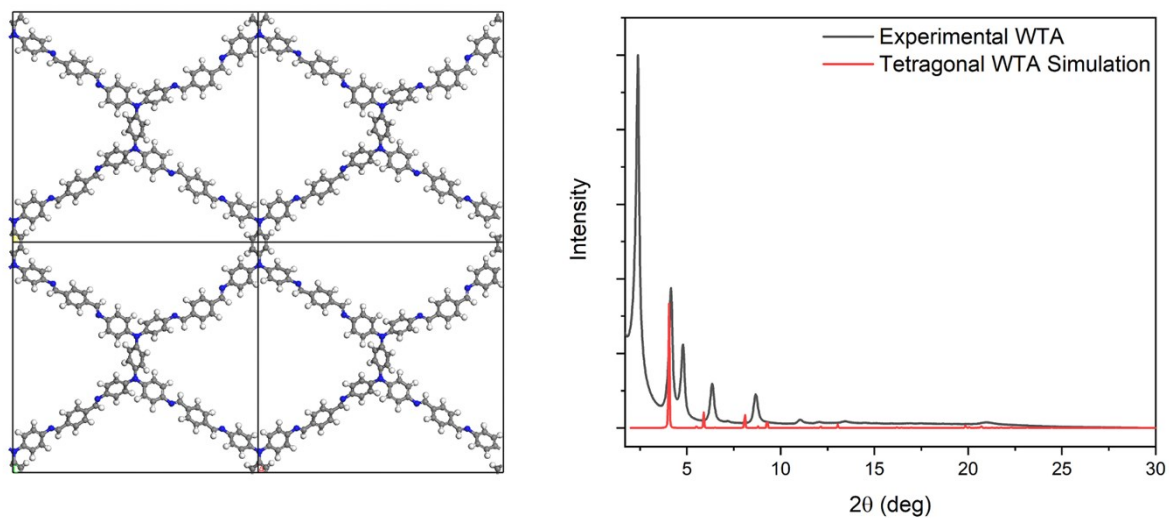


Figure S2: Simulated tetragonal structure of WTA and the corresponding calculated PXR D pattern vs. the experimental pattern.

Simulated tetragonal structure of WBDT

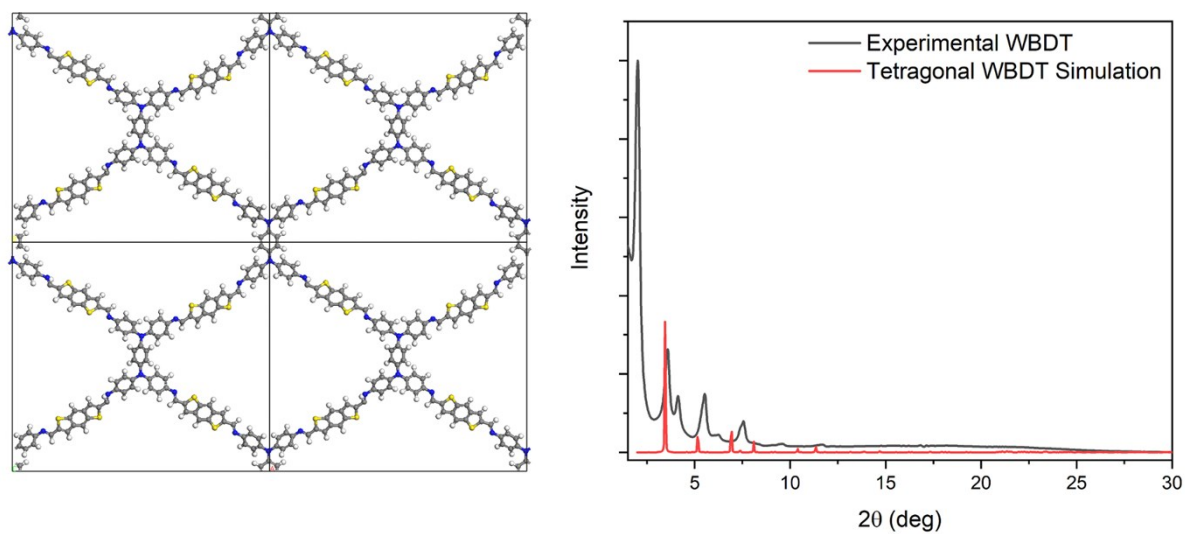


Figure S3: Simulated tetragonal structure of WBDT and the corresponding calculated PXR D pattern vs. the experimental pattern.

Hexagonal kagome vs. kagome-like arrangement of WTA

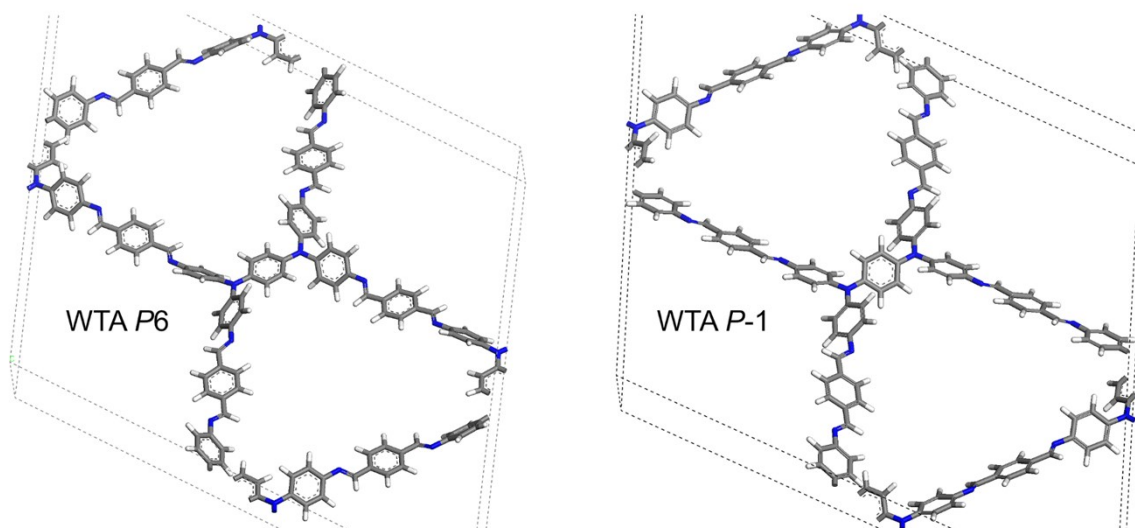


Figure S4: Representation of the geometric arrangement of the central **W** unit in WTA in a hexagonal $P6$ symmetry and in $P-1$ symmetry.

Hexagonal kagome vs. kagome-like arrangement of WBDT

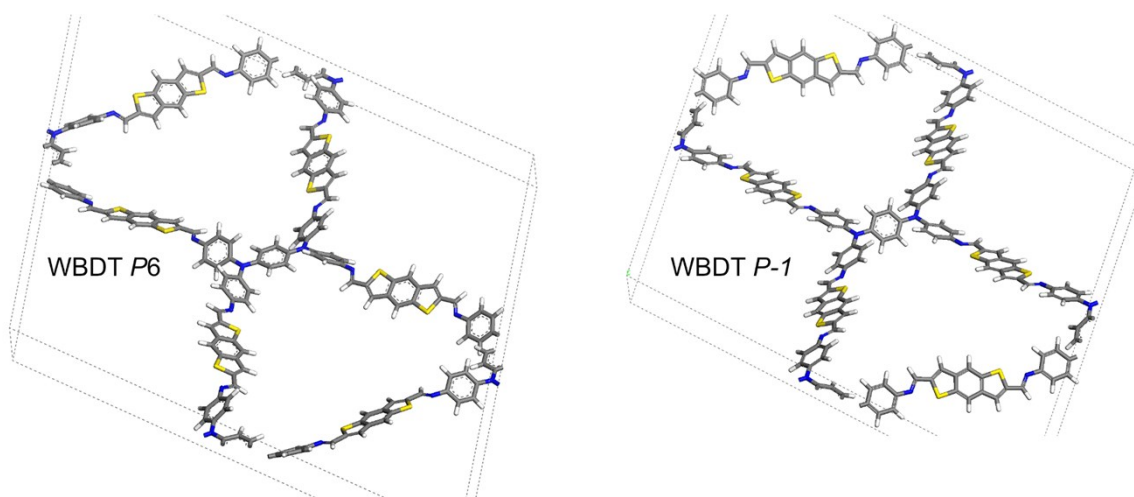


Figure S5: Representation of the geometric arrangement of the central **W** unit in WBDT in a hexagonal $P6$ symmetry and in $P-1$ symmetry.

Pore size distribution of WTA

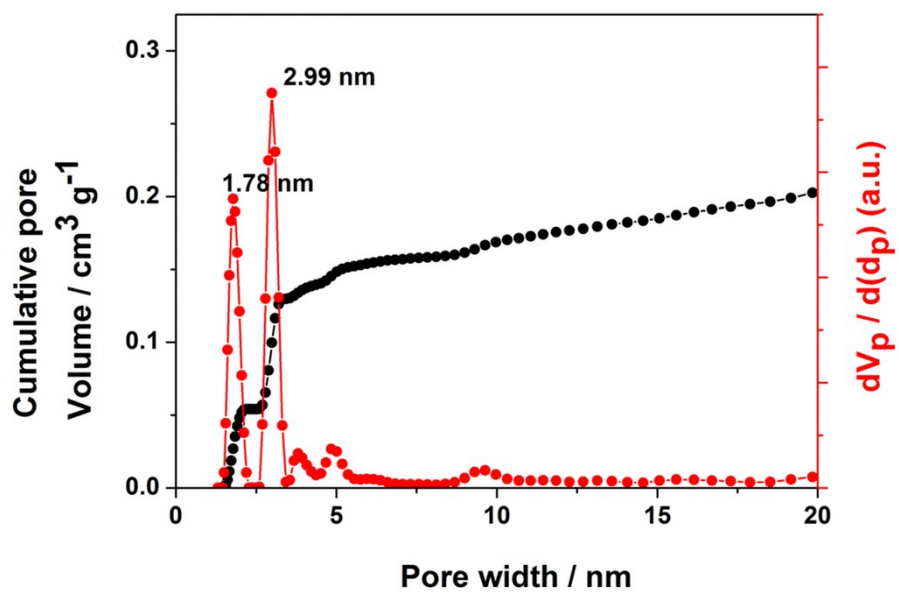


Figure S6: Pore size distribution and cumulative pore volume profiles of WTA obtained by QSDFT calculations on the N_2 adsorption curve.

Pore size distribution of WBDT

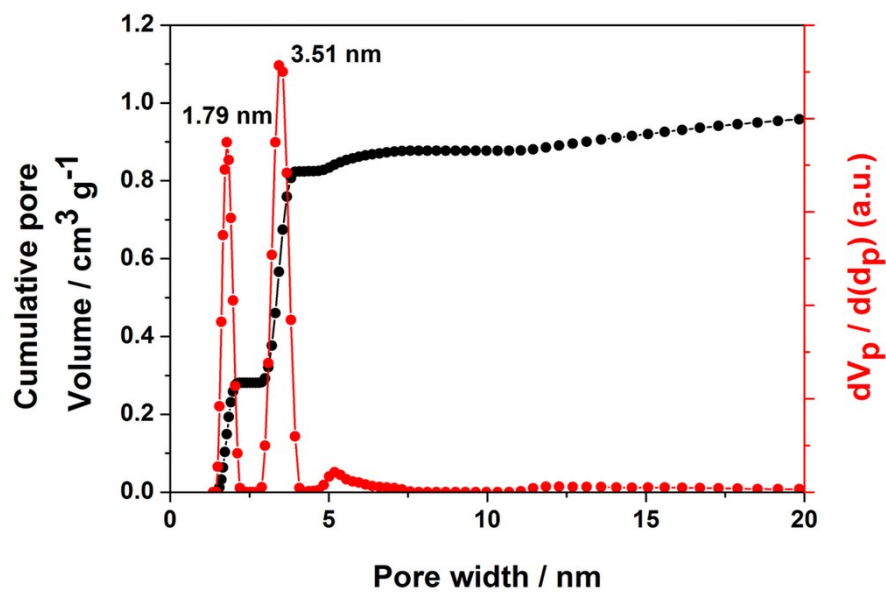


Figure S7: Pore size distribution and cumulative pore volume profiles of WBDT obtained by QSDFT calculations on the N_2 adsorption curve.

Tauc plot of WTA

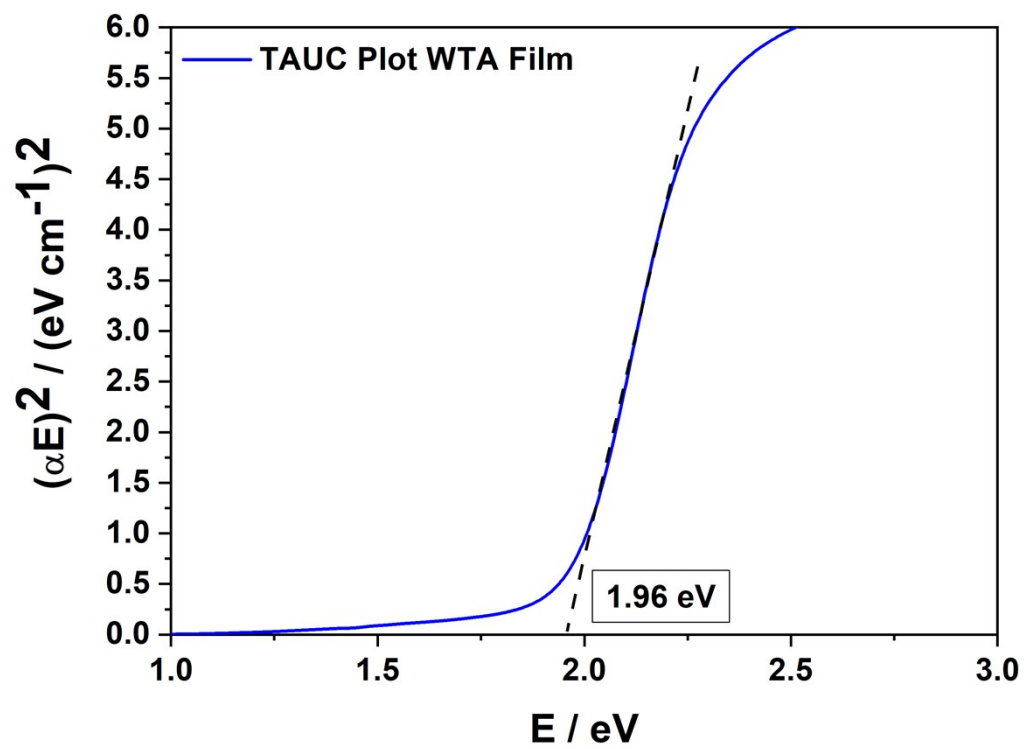


Figure S8: Tauc plot of the UV-vis absorption data of WTA.

Tauc plot of WBDT

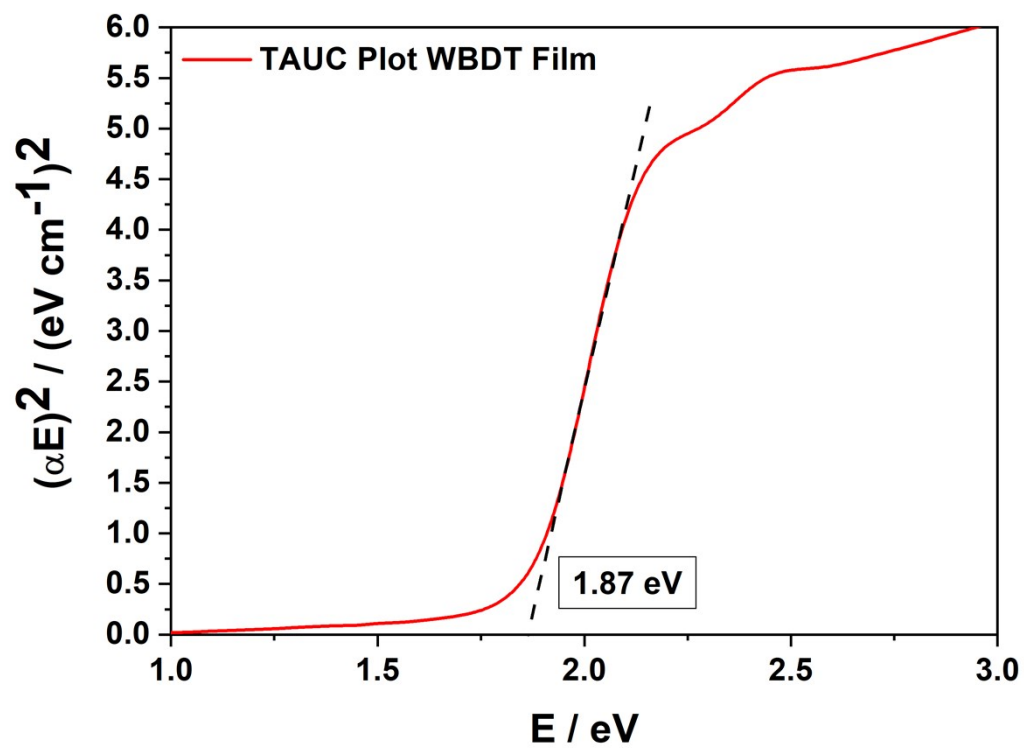


Figure S9: Tauc plot of the UV-vis absorption data of WBDT.

TCSPC decay data for WTA

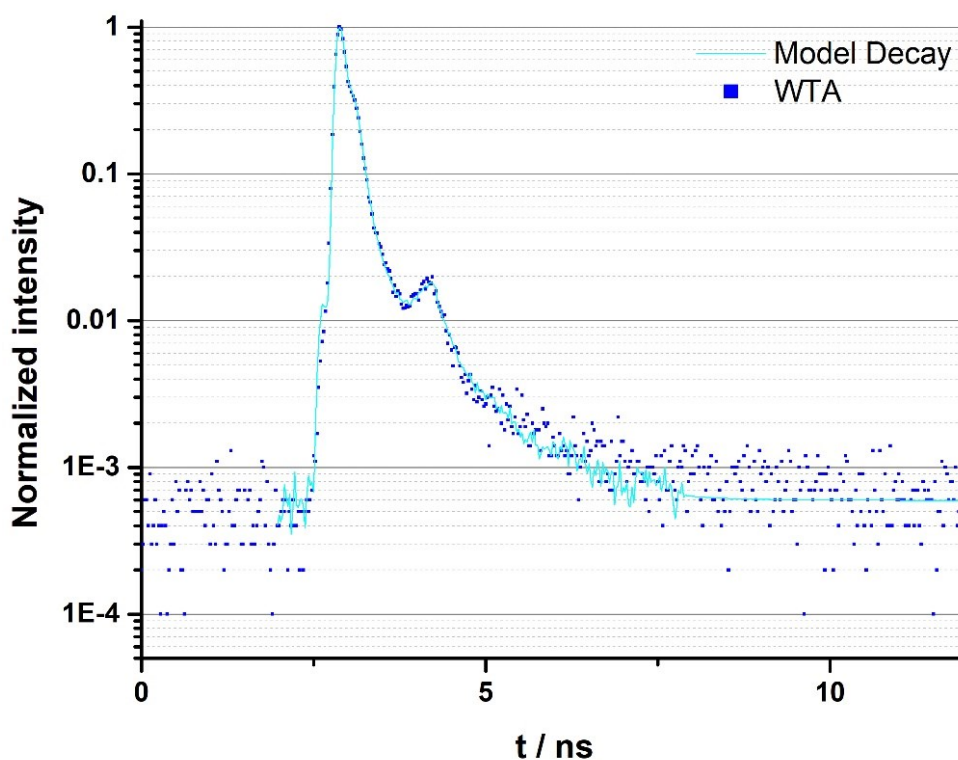


Figure S10: PL decay of WTA COF excited at 378 nm and measured at the maximum of the PL emission at 640 nm. Experimental decay: blue dots, biexponential fit of the decay: cyan line.

Table S2: PL decay times of WTA COF shown above. The given errors are uncertainties from the fit and hence do not reflect the real time-resolution of the setup. The latter is limited by the laser pulse duration of around 100 ps.

	τ / ns	error / ns	fractional intensity / %
τ_1	0.726	± 0.04	17.3
τ_2	0.100	± 0.003	82.7

TCSPC PL decay data for WBDT

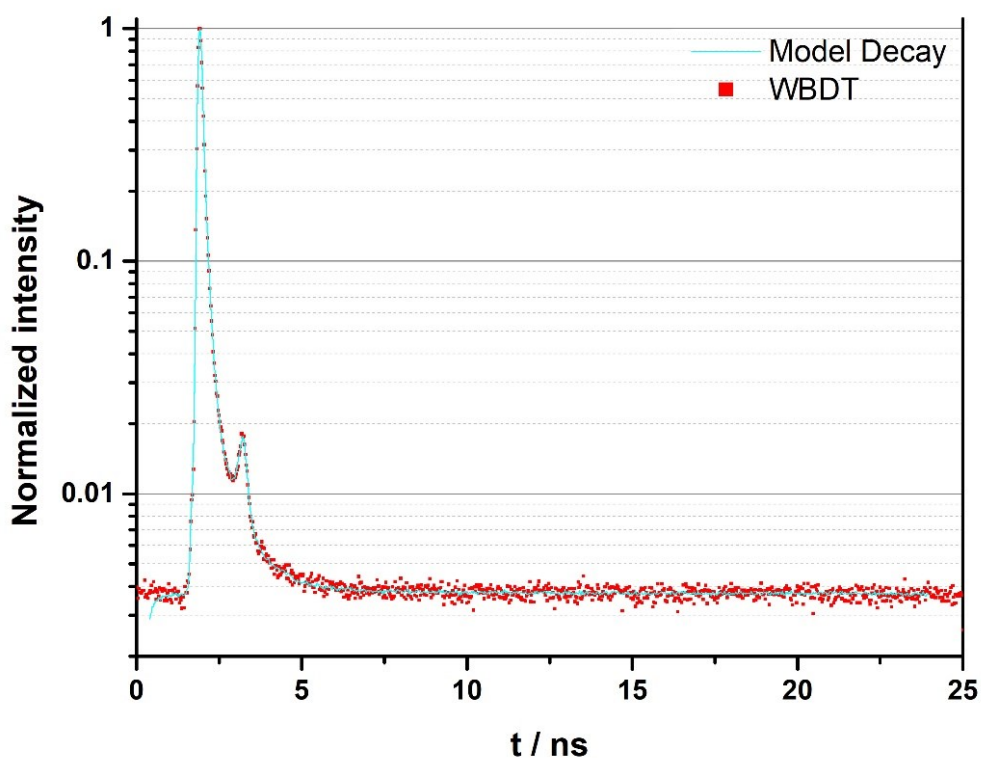


Figure S11: PL decay of WBDT COF excited at 378 nm and measured at the maximum of the PL emission at 675 nm. Experimental decay: red dots, biexponential fit of the decay: cyan line.

Table S3: PL decay times of WBDT COF shown above. The given errors are uncertainties from the fit and hence do not reflect the real time-resolution of the setup. The latter is limited by the laser pulse duration of around 100 ps.

	τ / ns	error / ns	fractional intensity / %
τ_1	0.720	± 0.04	13.6
τ_2	0.127	± 0.002	86.4

F₄TCNQ dopant concentration

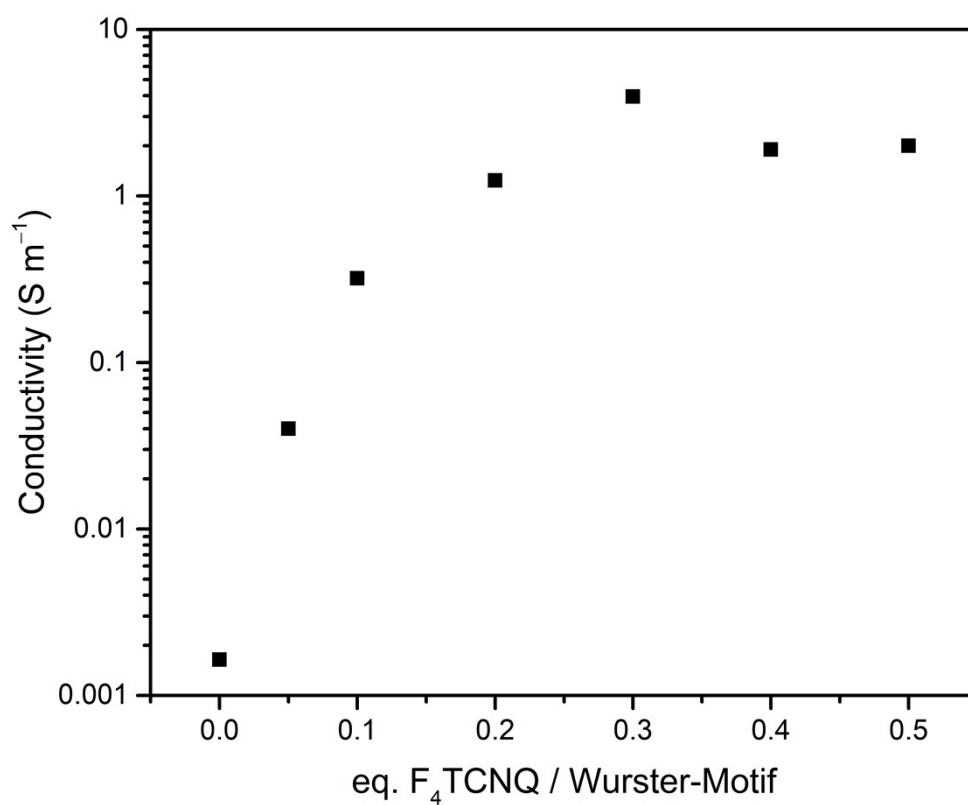


Figure S12: F₄TCNQ concentration-dependent electrical conductivities of WBDT.

PXRD of pristine WBDT vs. F₄TCNQ-doped WBDT

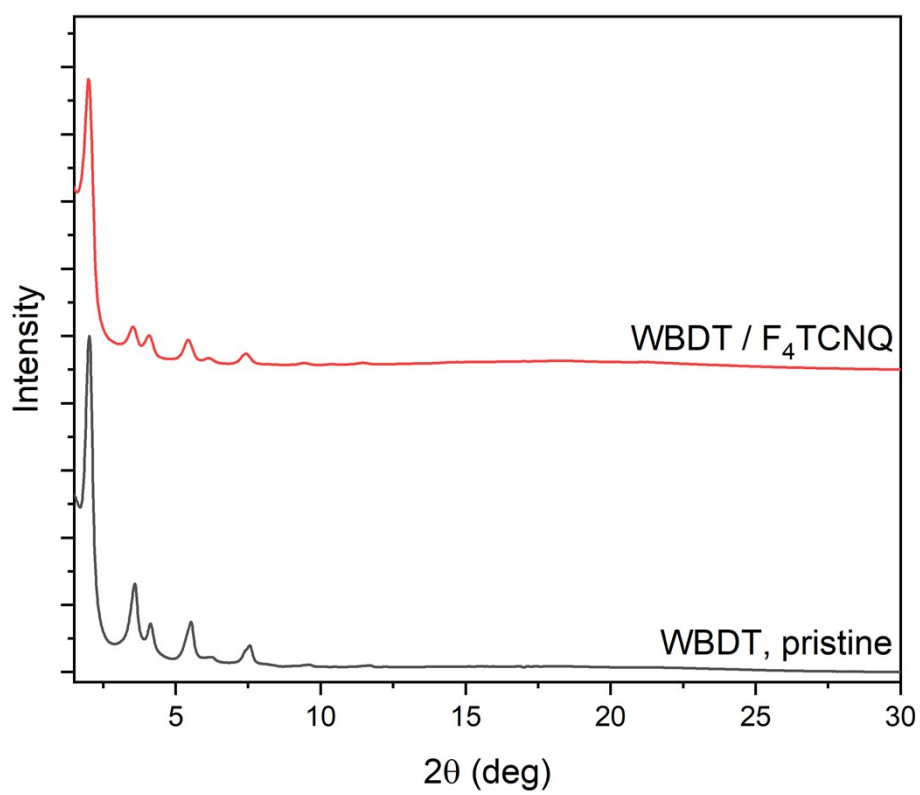


Figure S13: PXRD of pristine WBDT in comparison to F₄TCNQ-doped WBDT.

Electrical Conductivity

Table S4: Summary of electrical conductivity data of reported examples of doped Covalent Organic Frameworks.

Entry	Doped COF system (COF/dopant)	Room temperature conductivity (S/m)	Reference
1	WBDT / F ₄ TCNQ	3.67	Present work
2	TANG-COF / iodine	0.2 (air) 1 (vacuum)	ref. ²
3	COF-DL229 / iodine	1.5	ref. ³
4	JUC-518 / iodine	2.7×10^{-2} 1.4 (at 120 °C)	ref. ⁴
5	COF-DC-8 / iodine	around 2.5	ref. ⁵
6	TTF-COF / iodine	0.28	ref. ⁶

EPR quantification

To quantify the signal intensity of the EPR data, an α,γ -bis-diphenylene- β -phenyl allyl (BDPA) specimen was used as reference. The quantified data in Table S4 were obtained using Equation S1:

$$S.1 \quad N = \frac{[\text{total spin number}]}{(N_A m) / M_{u.c.}}$$

N is the number of radicals per unit cell, N_A the Avogadro constant, m the mass of investigated sample and $M_{u.c.}$ molar mass of WBDT (2679.39 g/mol) or WTA (2006.36 g/mol) unit cell.

Table S5: Overview of the total spin number and the calculated quantity of radicals for WTA and WBDT COF.

COF SYSTEM	TOTAL SPIN NUMBER	NUMBER OF RADICALS PER UNIT CELL
WTA, PRISTINE	$3.80 \cdot 10^{15}$	$2.53 \cdot 10^{-3}$
WTA / F ₄ TCNQ	$3.31 \cdot 10^{17}$	$2.21 \cdot 10^{-1}$
WBDT, PRISTINE	$2.72 \cdot 10^{15}$	$2.42 \cdot 10^{-3}$
WBDT / F ₄ TCNQ	$3.83 \cdot 10^{17}$	$3.40 \cdot 10^{-1}$
WBDT / SbCl ₅	$5.82 \cdot 10^{17}$	$5.18 \cdot 10^{-1}$
WBDT / IODINE	$3.70 \cdot 10^{17}$	$3.29 \cdot 10^{-1}$

Structural parameters of WTA

Unit Cell Parameters (*P*-1)

$a = 42.12$, $b = 42.82$, $c = 4.00$ Å

$\alpha = 91.3^\circ$, $\beta = 86.7^\circ$, $\gamma = 118.8^\circ$

Table S6: Fractional coordinates for WTA.

N1	N	0.56807	100.117	0.47259
C2	C	0.53414	100.065	0.48675
C3	C	0.50375	0.97391	0.66456
H4	H	0.50603	0.95338	0.80155
C5	C	0.47045	0.97327	0.67718
H6	H	0.44783	0.95221	0.82277
N7	N	0.57398	0.87287	0.50853
C8	C	0.56912	0.96878	0.47503
C9	C	0.54211	0.93803	0.32626
H10	H	0.52029	0.93912	0.19965
C11	C	0.54268	0.90605	0.33261
H12	H	0.52125	0.88312	0.20962
C13	C	0.57069	0.90348	0.48614
C14	C	0.5979	0.93435	0.63096
H15	H	0.61969	0.9329	0.75493
C16	C	0.59712	0.9662	0.62746
H17	H	0.61844	0.98932	0.74836
C18	C	0.55091	0.84221	0.39954
H19	H	0.52575	0.83712	0.27411
C20	C	0.39932	0.96613	0.53681
C21	C	0.36758	0.96295	0.70525
H22	H	0.36795	0.98565	0.83773
C23	C	0.33546	0.93107	0.70855
H24	H	0.31119	0.92925	0.84221
C25	C	0.33339	0.90089	0.54395
C26	C	0.36533	0.90376	0.38211
H27	H	0.3654	0.88103	0.2532
C28	C	0.39746	0.9357	0.37839
H29	H	0.42153	0.93696	0.24628
N30	N	0.29973	0.87024	0.56212
C31	C	0.29195	0.84209	0.38907
H32	H	0.31153	0.83958	0.20396
N33	N	0.56395	0.567	0.48736
C34	C	0.53201	0.53359	0.49375

C35	C	0.46968	0.49584	0.34229
H36	H	0.44645	0.49326	0.21118
C37	C	0.50088	0.5286	0.33649
H38	H	0.50093	0.55047	0.20148
N39	N	0.30219	0.43331	0.55131
C40	C	0.40189	0.43175	0.52473
C41	C	0.39694	0.45865	0.68764
H42	H	0.41926	0.48021	0.81528
C43	C	0.36381	0.45817	0.69159
H44	H	0.3606	0.47931	0.82062
C45	C	0.33404	0.4309	0.53396
C46	C	0.33865	0.40346	0.37841
H47	H	0.31631	0.38147	0.25431
C48	C	0.37189	0.40404	0.37326
H49	H	0.37461	0.38266	0.24415
C50	C	0.27393	0.41352	0.38746
H51	H	0.2721	0.3922	0.21113
C52	C	0.24218	0.41882	0.42695
C53	C	0.2441	0.44806	0.60843
C54	C	0.21416	0.45334	0.64861
H55	H	0.21614	0.47615	0.79332
C56	C	0.1812	0.42968	0.50774
C57	C	0.17929	0.40049	0.32536
C58	C	0.20925	0.39517	0.28567
H59	H	0.20728	0.37236	0.141
C60	C	0.56117	0.59855	0.49227
C61	C	0.58769	0.62956	0.32652
H62	H	0.6109	0.62966	0.18808
C63	C	0.58488	0.66048	0.33234
H64	H	0.60561	0.68398	0.1957
C65	C	0.55477	0.66114	0.49619
C66	C	0.52771	0.63	0.65446
H67	H	0.50436	0.6302	0.78744
C68	C	0.53133	0.59961	0.65921
H69	H	0.51028	0.57618	0.79328
N70	N	0.54956	0.69079	0.48322
C71	C	0.57435	0.72227	0.54939
H72	H	0.60122	0.72778	0.6412
C73	C	0.56827	0.75276	0.51297
C74	C	0.53712	0.74889	0.3638
C75	C	0.53154	0.77787	0.32634
H76	H	0.50726	0.77438	0.2061
C77	C	0.55682	0.81171	0.43806
C78	C	0.58791	0.81552	0.58827
C79	C	0.59361	0.7866	0.62375
H80	H	0.61792	0.79007	0.74324

N81	N	0.00549	0.56852	0.52085
C82	C	0.00281	0.53436	0.51062
C83	C	0.02825	0.52794	0.32203
H84	H	0.05046	0.54926	0.17518
C85	C	0.02549	0.49443	0.31146
H86	H	0.04564	0.49075	0.15642
N87	N	0.14367	0.69002	0.45561
C88	C	0.04004	0.59919	0.50487
C89	C	0.07015	0.59901	0.6395
H90	H	0.06712	0.57512	0.76159
C91	C	0.10417	0.62885	0.61926
H92	H	0.12706	0.62815	0.72885
C93	C	0.10898	0.6606	0.47822
C94	C	0.0791	0.66103	0.3429
H95	H	0.08254	0.68501	0.21822
C96	C	0.04542	0.63068	0.3514
H97	H	0.023	0.63165	0.2354
C98	C	0.14971	0.72113	0.54655
H99	H	0.12786	0.72613	0.66572
C100	C	0.19336	0.78465	0.64917
C101	C	0.18599	0.75181	0.50591
C102	C	0.21408	0.74922	0.32187
H103	H	0.20856	0.72385	0.20647
C104	C	0.24832	0.77851	0.28171
C105	C	0.25583	0.81126	0.42841
C106	C	0.22774	0.81378	0.61346
H107	H	0.23332	0.83913	0.72998
C108	C	0.02644	0.42832	0.45812
C109	C	0.02764	0.3996	0.2922
H110	H	0.00379	0.37937	0.17051
C111	C	0.05909	0.39671	0.276
H112	H	0.0594	0.37425	0.14391
C113	C	0.09077	0.42226	0.42357
C114	C	0.08981	0.45138	0.58384
H115	H	0.1137	0.47222	0.70061
C116	C	0.0583	0.45413	0.60195
H117	H	0.05851	0.47682	0.73349
N118	N	0.12111	0.41718	0.39226
C119	C	0.14995	0.43565	0.55347
H120	H	0.15284	0.45693	0.73506
H121	H	0.26959	0.46655	0.72058
H122	H	0.15385	0.38198	0.21265
H123	H	0.51734	0.72269	0.27437
H124	H	0.60763	0.84171	0.67857
H125	H	0.17183	0.78714	0.79505
H126	H	0.26976	0.77609	0.13374

Structural parameters of WBDT

Unit Cell Parameters (*P*-1)

$a = 50.55$, $b = 49.64$, $c = 3.93 \text{ \AA}$

$\alpha = 102.3^\circ$, $\beta = 82.2^\circ$, $\gamma = 120.8^\circ$

Table S7: Fractional coordinates for WBDT.

N1	N	0.55374	0.99687	-	0.60032
C2	C	0.52694	0.99856	-	0.55079
C3	C	0.50431	0.9766	-	0.37176
H4	H	0.50775	0.95834	-	0.26936
C5	C	0.47802	0.97806	-	0.32231
H6	H	0.4611	0.96102	-	0.17751
S7	S	0.56531	0.84115	-	0.48225
N8	N	0.55291	0.88478	-	0.64731
C9	C	0.55336	0.96869	-	0.61445
C10	C	0.52759	0.94343	-	0.72101
H11	H	0.50758	0.94559	-	0.79244
C12	C	0.5273	0.91583	-	-0.7372
H13	H	0.50692	0.89656	-	0.81845
C14	C	0.55252	0.91227	-	0.64593
C15	C	0.57803	0.93733	-	0.53323
H16	H	0.59771	0.93479	-	0.45944
C17	C	0.57861	0.96509	-	0.52136
H18	H	0.59869	0.98428	-	0.43224

C19	C	0.53669	0.86342	-	0.82589
H20	H	0.52182	0.86542	-	1.00479
C21	C	0.53994	0.83649	-	0.77446
C22	C	0.52782	0.80856	-	0.89572
H23	H	0.51147	0.80152	-	1.07651
C24	C	0.41887	0.97625	-	0.34965
C25	C	0.39763	0.97539	-	0.15227
H26	H	0.40252	0.99595	-	0.03827
C27	C	0.3711	0.94893	-	0.09736
H28	H	0.35549	0.94916	-	0.05724
C29	C	0.36489	0.92251	-	0.23177
C30	C	0.38506	0.92317	-	0.43853
H31	H	0.38111	0.90359	-	0.56207
C32	C	0.41181	0.9496	-	0.49561
H33	H	0.42776	0.95014	-	0.65923
S34	S	0.2414	0.8349	-	0.32396
N35	N	0.31609	0.88778	-	0.0643
C36	C	0.2983	0.86168	-	-0.0272
H37	H	0.30467	0.85348	-	0.23181
C38	C	0.2683	0.83701	-	0.06684
C39	C	0.25625	0.81046	-	0.08154
H40	H	0.26749	0.80476	-	0.24972
N41	N	0.55388	0.55424	-	0.49343
C42	C	0.52687	0.52702	-	0.49671
C43	C	0.47469	0.49789	-	0.36069
H44	H	0.45507	0.49603	-	0.24683
C45	C	0.5014	0.52471	-	-0.3578
H46	H	0.50272	0.54391	-	-

				0.24176
S47	S	0.28988	0.45744	0.32772
N48	N	0.33435	0.44555	0.49764
C49	C	0.41826	0.44603	0.49583
C50	C	0.41405	0.4695	0.35706
H51	H	0.4328	0.48814	0.24117
C52	C	0.38624	0.46891	0.36173
H53	H	0.38306	0.48715	0.25415
C54	C	0.36183	0.44526	0.50778
C55	C	0.3661	0.42192	0.64671
H56	H	0.34755	0.40313	0.75992
C57	C	0.39377	0.42232	0.64061
H58	H	0.39708	0.40427	0.75278
C59	C	0.31278	0.42949	0.67778
H60	H	0.31472	0.41507	0.86249
C61	C	0.28571	0.43224	0.62199
C62	C	0.25781	0.41973	0.74669
H63	H	0.25118	0.40335	0.92866
C64	C	0.23872	0.43064	0.60577
C65	C	0.25341	0.45192	0.36921
C66	C	0.2386	0.46534	0.20682
H67	H	0.24976	0.48158	0.02454
C68	C	0.20907	0.45786	0.27955
C69	C	0.19442	0.43661	0.51632
C70	C	0.20916	0.42306	0.67776
H71	H	0.198	0.40686	0.86042
C72	C	0.55294	0.58182	-
C73	C	0.57562	0.60613	-
H74	H	0.59343	0.60302	0.21865
C75	C	0.57538	0.63351	-
H76	H	0.59341	0.65192	0.21386
C77	C	0.55242	0.63763	-
C78	C	0.52974	0.61335	0.63476
H79	H	0.51176	0.61633	-0.7501
C80	C	0.52982	0.58584	-
H81	H	0.51199	0.56724	0.76009
S82	S	0.53925	0.70892	-
				0.67797

N83	N	0.55166	0.66488	-	0.49642
C84	C	0.56703	0.68657	-	0.31776
H85	H	0.58113	0.68494	-	0.12895
C86	C	0.5641	0.71344	-	0.38114
C87	C	0.57644	0.74152	-	-0.2628
H88	H	0.59258	0.74843	-	0.08024
C89	C	0.56572	0.76043	-	0.41147
C90	C	0.5447	0.74543	-	0.64619
C91	C	0.53144	0.76003	-	0.81534
H92	H	0.5154	0.74858	-	-0.9964
C93	C	0.53896	0.78974	-	-0.7516
C94	C	0.56007	0.80474	-	0.51755
C95	C	0.57336	0.79018	-	0.34886
H96	H	0.58939	0.80158	-	0.16763
C97	C	0.02094	0.52108	-	0.69036
H98	H	0.0371	0.53714	-	0.84593
C99	C	0.02231	0.49469	-	0.64116
H100	H	0.03943	0.4902	-	0.75515
S101	S	0.15423	0.70685	-	-0.125
N102	N	0.09957	0.66077	-	0.10778
C103	C	0.02281	0.58013	-	0.32738
C104	C	0.05129	0.5873	-	0.43623
H105	H	0.05352	0.57185	-	0.58489
C106	C	0.07644	0.6139	-	0.36165
H107	H	0.09834	0.61897	-	0.44748
C108	C	0.07402	0.63416	-	0.17333
C109	C	0.04549	0.62711	-	0.06862
H110	H	0.04269	0.64247	-	0.07407
C111	C	0.02038	0.60069	-	0.14267

C112	C	0.10041	0.67784	0.10428
H113	H	0.08156	0.6719	0.25709
C114	C	0.12833	0.70534	0.12721
C115	C	0.13851	0.73048	0.2955
H116	H	0.12464	0.73349	0.45343
C117	C	0.16848	0.75241	0.22041
C118	C	0.18027	0.74227	- 0.00739
C119	C	0.20902	0.76011	- 0.11437
H120	H	0.21769	0.75207	- 0.29008
C121	C	0.22653	0.78857	0.00259
C122	C	0.21478	0.79878	0.2277
C123	C	0.1859	0.78078	0.33872
H124	H	0.17683	0.78853	0.51371
C125	C	0.03143	0.44681	0.4072
C126	C	0.03419	0.42138	0.51286
H127	H	0.01429	0.40148	0.59831
C128	C	0.0618	0.42149	0.51472
H129	H	0.06382	0.40174	0.5978
C130	C	0.08748	0.44668	0.40428
C131	C	0.08487	0.47222	0.30341
H132	H	0.10473	0.49238	0.22577
C133	C	0.05736	0.47233	0.30539
H134	H	0.05555	0.49236	0.2245
S135	S	0.15826	0.43169	0.56375
N136	N	0.11454	0.44552	0.41008
C137	C	0.13589	0.46102	0.22625
H138	H	0.13391	0.4757	0.04395
C139	C	0.16253	0.45727	0.27273
C140	C	0.19018	0.46922	0.14302
H141	H	0.19686	0.48574	- 0.03768
N142	N	0.99684	1.55341	0.59983
C143	C	0.99869	1.52683	0.55075
H144	H	0.99841	1.59543	0.9461

References

- (1) Aradi, B.; Hourahine, B.; Frauenheim, T. DFTB+, a sparse matrix-based implementation of the DFTB method. *J. Phys. Chem. A* **2007**, *111*, 5678–5684.
- (2) Lakshmi, V.; Liu, C.; Rao, M.R.; Chen, Y.; Fang, Y.; Dadvand, A.; Hamzehpoor, E.; Sakai-Otsuka, Y.; Stein, R.S.; Perepichka, D.F. A Two-Dimensional Poly(azatriangulene) Covalent Organic Framework with Semiconducting and Paramagnetic States. *J. Am. Chem. Soc.* **2020**, *142*, 2155-2160.
- (3) Wang, C.; Wang, Y.; Ge, R.; Song, X.; Xing, X.; Jiang, Q.; Lu, H.; Hao, C.; Guo, X.; Gao, Y.; Jiang, D., A 3D Covalent Organic Framework with Exceptionally High Iodine Capture Capability. *Chem. Eur. J.* **2018**, *24*, 585-589.
- (4) Li, H.; Chang, J.; Li, S.; Guan, X.; Li, D.; Li, C.; Tang, L.; Xue, M.; Yan, Y.; Valtchev, V.; Qiu, S.; Fang, Q., Three-Dimensional Tetrathiafulvalene-Based Covalent Organic Frameworks for Tunable Electrical Conductivity. *J. Am. Chem. Soc.* **2019**, *141*, 13324-13329.
- (5) Meng, Z.; Stolz, R. M.; Mirica, K. A., Two-Dimensional Chemiresistive Covalent Organic Framework with High Intrinsic Conductivity. *J. Am. Chem. Soc.* **2019**, *141*, 11929-11937.
- (6) Cai, S.-L.; Zhang, Y.-B.; Pun, A. B.; He, B.; Yang, J.; Toma, F. M.; Sharp, I. D.; Yaghi, O. M.; Fan, J.; Zheng, S.-R.; *et al.* Tunable electrical conductivity in oriented thin films of tetrathiafulvalene-based covalent organic framework. *Chem. Sci.* **2014**, *5*, 4693–4700.